CAAP Quarterly Report

06/30/2025

Project Name: A Novel Reliability-Based Approach for Assessing Pipeline Cathodic Protection (CP) Systems in External Corrosion Management

Contract Number: 693JK32350002CAAP

Prime University: Marquette University

Prepared By: Qindan Huang, Qindan.huang@marquette.edu, 414-288-6670; Qixi Zhou, qzhou@uakron.edu, 330-972-7159

Reporting Period: 04/01/2025-06/30/2025

Project Activities for Reporting Period:

The research team has been working on Task 3 (DC interference lab testing) and Task 4 (probabilistic defect growth modeling).

Task 3 Corrosion behavior under stray current interference

During this report perior, we have started tracking the DC interference corrosion behavior of X60 using Tafel, Chronopotentiometry, and surface morphology. Three levels of DC interference (0.1, 1, and 10 A/m^2), two interference periods (1/10, 1/2, and 9/10), and two durations (1 and 3 days) were applied by Gamry Reference 600 Chronopotentiometry mode.

Tafel testing

Figure 1 shows the Tafel plot for X60 steel under 1:10 interference period, different DC interferences: a) 0.1 A/m^2; b) 1 A/m^2; c) 10 A/m^2, and different durations. The corrosion current and the corrosion potential increase with time, which indicates that the corrosion products on the metal surface also increase with time. Table 1 shows the corrosion rate of X60 derived from Tafel plots. The corrosion rate decreases with DC interference, indicating that the corrosion product on the surface grows in response to DC interference and provides protection.

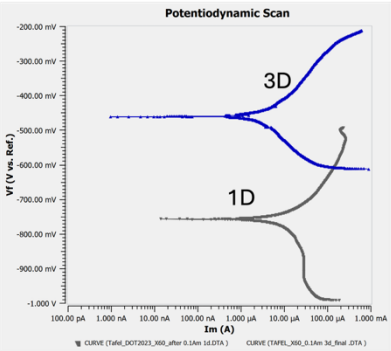

a) 0.1A/m^2

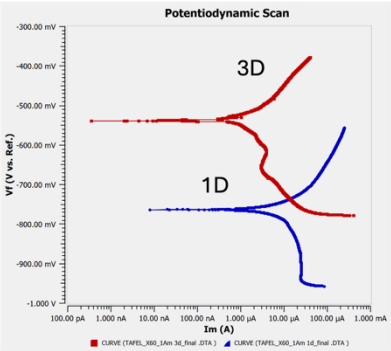

b) 1A/m^2

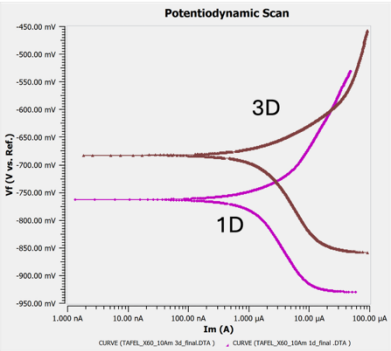

c) 10A/m^2

Figure 1. Tafel plot for X60 steel under 1:10 interference period, different DC interference: a) 0.1 A/m^2; b) 1 A/m^2; c) 10 A/m^2, and different durations.

Table 1. Corrosion rate of X60 derived from Tafel plots under different DC interference, interference period, and durations.

DC interference (A/m^2)	interference period	duration/day	Corrosion rate/mpy
0.1	1/10	3	2.768
0.1	1/2	3	5.914
0.1	9/10	3	7.435
0.1	1/10	1	19.72
0.1	1/2	1	23.67
0.1	9/10	1	20.45
1	1/10	3	2.89
1	1/2	3	3.638
1	9/10	3	1.234
1	1/10	1	13.72
1	1/10	1	15.08
1	1/2	1	8.813
1	9/10	1	0.617
10	1/10	3	0.834
10	1/2	3	0.804
10	9/10	3	In process
10	1/10	1	1.607
10	1/10	1	2.234
10	1/2	1	0.566
10	9/10	1	0.531
10	9/10	1	0.847
10	9/10	1	0.587

Chronopotentiometry

We also use chronopotentiometry to track the DC potential change during different DC interference conditions, as shown in Figure 2. The interference period is considered one of the key parameters in the study. Figure 3 shows the example of the DC interference current density in green and its corresponding DC potential in blue, which helps us better understand the existence of two lines in Figure 2.

In Figure 2, the bottom line represents the DC current density of 0 A/m^2, which corresponds to the metro stop condition. The top line depicts DC current density of 0.1 A/m^2, 1 A/m^2, and 10 A/m^2, which refers to the metro move condition. The top DC potential is -715 mV vs. SCE in Figure 2a, -600 mV vs. SCE in Figure 2b, and -400 mV vs. SCE in the early stage in Figure 2c. This indicates that the corrosion product accumulates on the metal surface along with the

increase of the DC current density. Also, a dramatic increase was observed in Figure 2c after 50ks, indicating that the reaction mechanism may abruptly change, causing severe potential fluctuations.

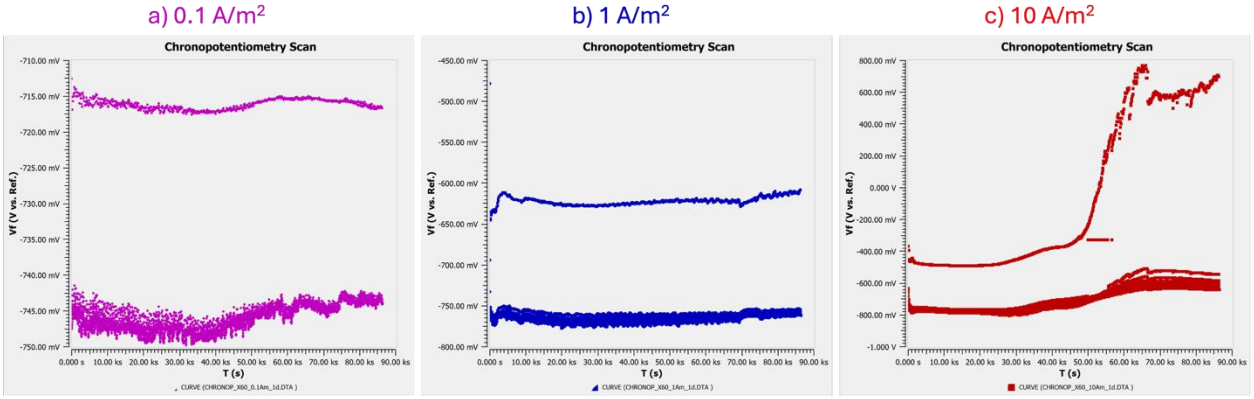

Figure 2. DC potential of X60 under 1 day, 1:10 interference period, and different DC interference current densities: a) 0.1 A/m^2; b) 1 A/m^2; c) 10 A/m^2.

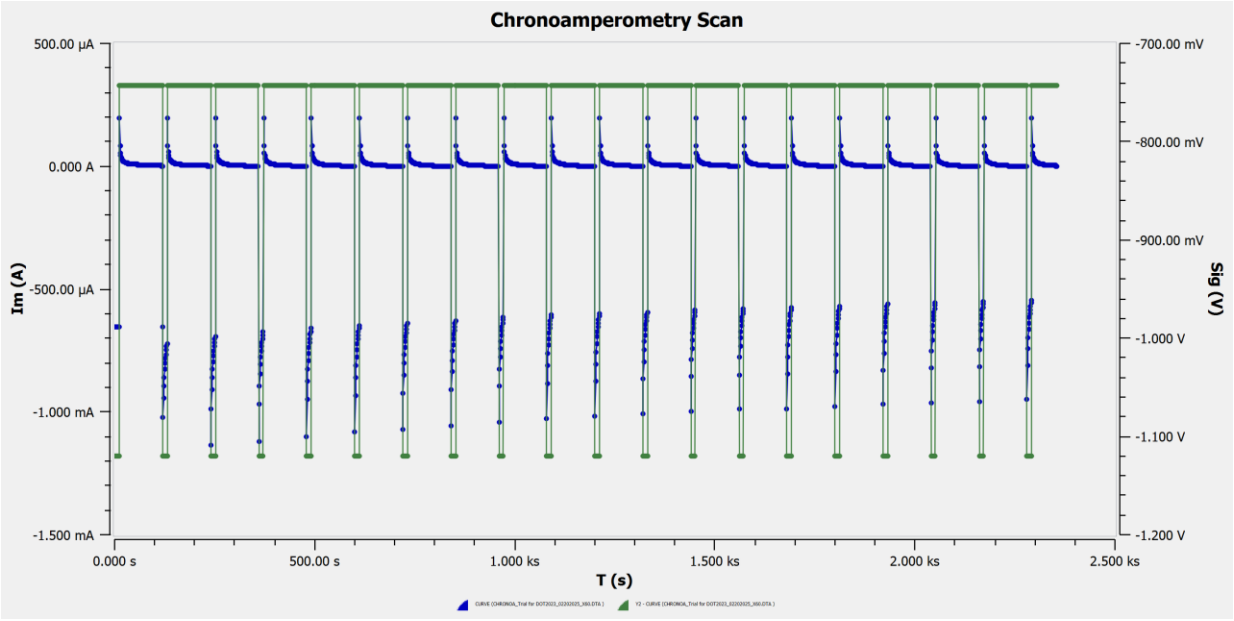

Figure 3. Example of DC interference current density (green) and its corresponding DC potential (blue).

Surface morphology

Figure 4 shows the surface morphology of X60 under 1:10 interference period, different DC interference, and durations. Under a low current density of 0.1 A/m^2, the surface appeared dark gray, with uniform and dense texture after 1 day. After 3 days, the surface turned tan, remaining relatively uniform overall. Under medium current density of 1 A/m^2, the surface became rougher, indicating enhanced reaction activity under medium current, with reaction products starting to accumulate on the surface after 1 day. After 3 days, yellow spots appeared, with abrupt color

changes in local areas. It demonstrates that under long-term medium current, local degradation occurred on the electrode surface. Under the high current density of 10 A/m^2, the surface was mottled with dense holes, and a yellowish corrosion zone appeared at the edge after 1 day. After 3 days, layered corrosion appeared and easy spalling. In conclusion, the higher the current density and the longer the action time, the more severe the electrochemical damage to the electrode surface.

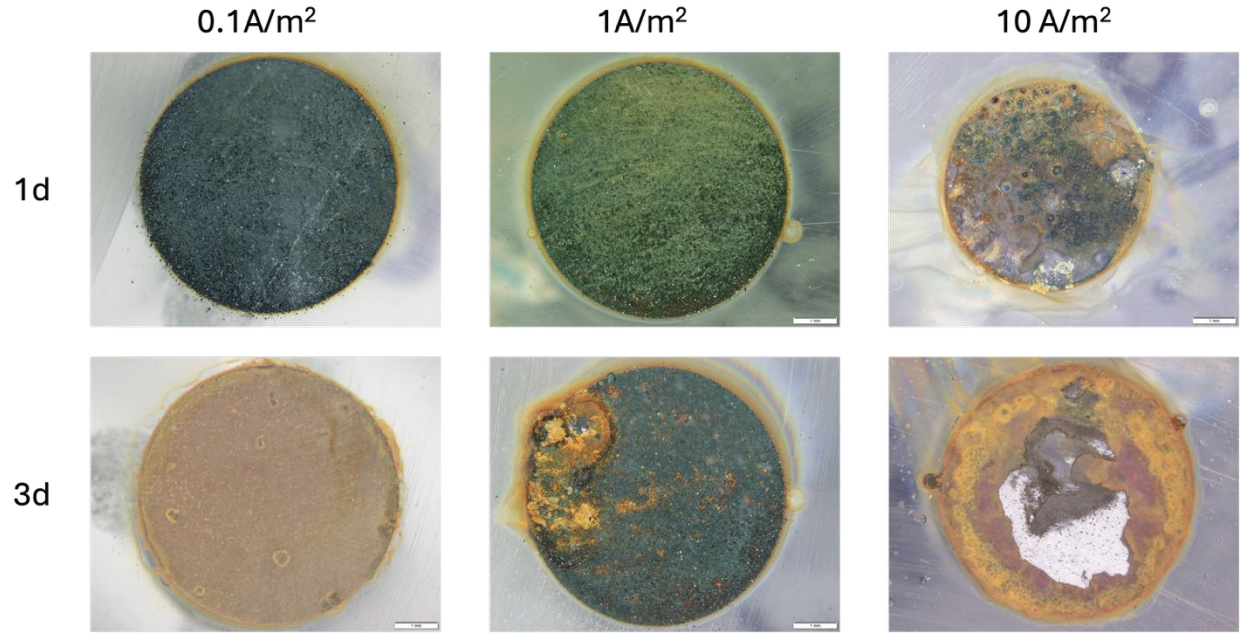

Figure 4. Surface morphology of X60 under 1:10 interference period, different DC interference, and durations.

Task 4 Probabilistic defect growth modeling

Corrosion Surface Area and Volume Growth Considering Measurement Error

The measurement error of ILI devices and their effect on the calculated defect area and volume are considered. According to ILI tool specifications provided by vendors, accuracy of the utilized tools is provided given morphology of an anomaly. For example, depth measurement accuracy is given in terms of 80% confidence interval of x% of the wall thickness. This means that depth measurement is uncertain and there is an 80% chance that the true depth is within the measured depth $\pm x$% of wall thickness. From this information, the uncertainty, i.e., standard deviation, of the measured depth can be obtained by assuming a distribution (e.g., Normal distribution). The measurement error for length or width, however, is usually given in terms of millimeter of the additive sizing error.

The uncertainty in depth, width, and length measurements should be propagated into the calculated area and volume of defects. One could adopt the first-order Taylor expansion to linearize the area and volume functions for simple calculation of the standard deviation of the functions. As an example, Eq. (1) shows the linearization of a function $f(x_1, x_2, x_3)$, using the first-order Taylor expansion around the point a_1, a_2, a_3:

$$f(x_1,x_2,x_3) \approx f(a_1,a_2,a_3) + \sum_{i=1}^{3} \frac{\partial f}{\partial x_i}(a_1,a_2,a_3)\cdot(x_i - a_i) \tag{1}$$

where $\frac{\partial f}{\partial x_i}(a_1,a_2,a_3)$ is the partial derivative of f with respect to x_i evaluated at a_1, a_2, a_3.

To linearize the area function, A, which is the product of width, W, and length, L, using the Taylor series expansion around the mean values of W and L, i.e., μ_W and μ_L, the above equation is used as follows:

$$A = W \cdot L \approx f(\mu_W,\mu_L) + \mu_L(W-\mu_W) + \mu_W(W-\mu_L) \approx \mu_W \cdot L + \mu_L \cdot W - \mu_W \cdot \mu_L \tag{2}$$

Therefore, the mean and standard deviation of area, i.e., μ_A and σ_W, assuming Normal distribution for width and length and independence of W and L, is obtained as follows:

$$\begin{aligned} \mu_A &= \mu_W \cdot \mu_L \\ \sigma_A &= \sqrt{\mu_W{}^2 \cdot \sigma_L{}^2 + \mu_L{}^2 \cdot \sigma_W{}^2} \end{aligned} \tag{3}$$

After estimating the uncertainty of the calculated area (or volume) of defects over different ILIs, the probability of area (or volume) positive growth over time can be estimated using:

$$P\left(Positve\ Growth\right) = P\left(A_2 > A_1\right) = \Phi\left(\frac{\mu_{A_2} - \mu_{A_1}}{\sqrt{\sigma_{A_2}^2 + \sigma_{A_1}^2}}\right) \tag{4}$$

Figure 5 shows the probability that the actual area of defects detected in the second ILI, A_2, of a pipe joint is greater than that in the first ILI, A_1, i.e., P(*Postive area growth*), when all the single metal loss (SML) and child features of a pipe joint are considered.

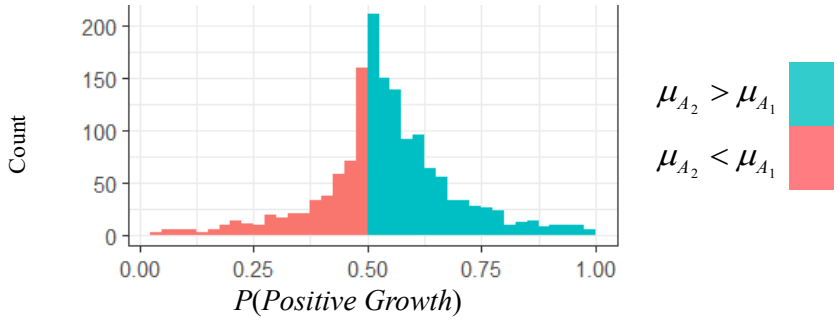

Figure 5. Probability of *positive* area growth over time

As shown in Figure 5, since Normal distributions are assumed for A_1 and A_2, for the joints where the measured A_2 is greater than the measured A_1, i.e., $\mu_{A_2} > \mu_{A_1}$, P(*Positive Growth*) lies in between 0.5 and 1, depending on the A_1 and A_2 distribution parameters. That is, when $\mu_{A_2} > \mu_{A_1}$, the P(*Positive Growth*) can sometimes be as low as 0.5, as opposed to the deterministic evaluation with no consideration of measurement errors resulting in 100% of positive growth. On the other hand, when $\mu_{A_2} < \mu_{A_1}$, the P(*Positive Growth*) can sometimes be as high as 0.5, while

in the deterministic evaluation it would be considered as 100% negative growth. This result shows the importance of considering ILI measurement error and probabilistic evaluation when evaluating the growth of area of defects within a joint over time.

In addition, using the same dataset as Figure 5, Figure 6 shows for higher values of mean area ratio, i.e., μ_{A_2} / μ_{A_1}, the probability of actual positive area growth over time, i.e., *P*(*Positive Growth*), is generally higher. However, the correlation is not always linear, as it depends on number of defects within a joint, Probability of Detection (POD), and sizing error. It is noted that in theory where $\mu_{A_2} = \mu_{A_1}$, *P*(*Positive Growth*) = 0.5. Moreover, Figure 6 below shows the effect of considering POD on *P*(*Positive Growth*) to be insignificant.

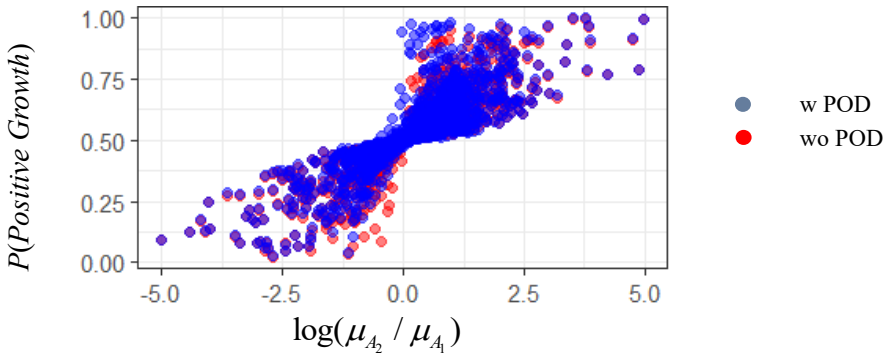

Figure 6. Probability of positive area growth over time versus mean area ratio

Predicting the Probability of Corrosion Occurrence on a Pipe Joint

In this section, the effect of all influencing factors on the occurrence of corrosion on pipe joints will be evaluated. Specifically, logistic regression analysis are carried out to develop a predictive model to predict the probability of corrosion occurrence within a pipe joint given the influencing factors. Such a model would help operators better understand and manage their assets and plan future in-line inspections more efficiently.

A subset of available pipe joints is selected where no corrosion was detected on the entire joint in the 1st inspection. These pipe joints are classified into two groups based on whether defects were detected in the 2nd inspection or not. If defects are detected in the 2nd inspection with a joint, the joint is labelled as Class 1, otherwise, it is labelled as Class 0. Therefore, binary logistic regression analysis is used to develop a model which predicts the probability of a pipe joint having corrosion in the next inspection given no corrosion in the 1st ILI. Undersampling technique was utilized so the total number of observations per Class is the same, and balanced dataset is used for model development purposes. Totally, 1,101 observations were used for each Class, results in 2,202 observations for both classes combined. Overall, 22 unique variables were currently used in the developed logistic model, and a detailed investigation on their "importance" and contribution on the accuracy of the model is ongoing.

Figure 7 shows the distribution of the predicted probability of having defects in the 2nd inspection obtained from the developed logistic model for two pipelines considered. An perfect

model would predict probability values of 1 and 0 for Class 1 and Class 0, respectively. As shown in Figure 7, a clear distinction between the distribution of probabilities for Class 1 and Class 0, i.e., the bule and red distributions, is shown. In particular, the majority of probability values are closer to 1 for Class 1 and the majority of probability values are closer to 0 for Class 0, signifying the good performance of the developed predicted model.

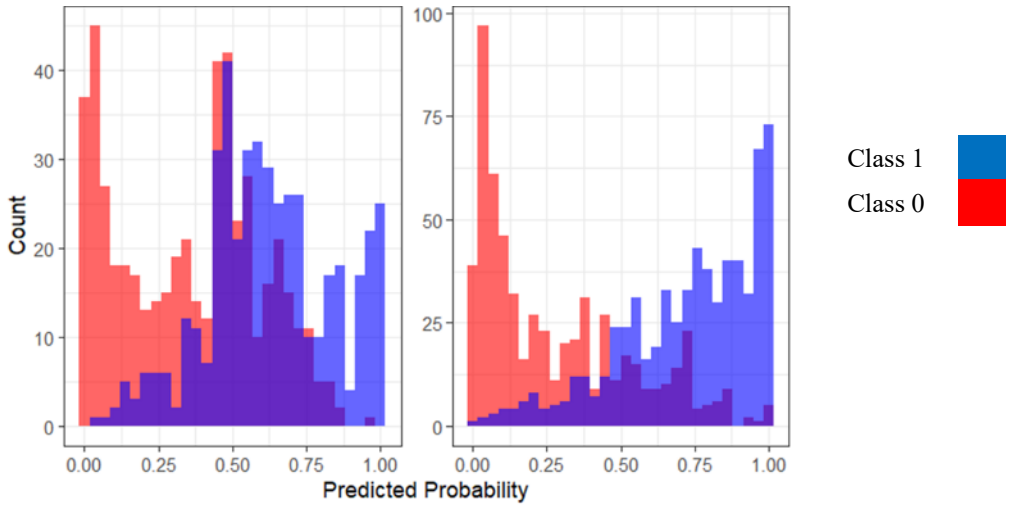

(a) Pipeline 1 (b) Pipeline 2

Figure 7. Predicted probability of having defect in the 2nd inspection

To check if the model prediction is biased (that is, the model is predicting one class with better accuracy than the other), the Root Mean Squared Error (*RMSE*) and Mean Absolute Error (*MAE*) values are calculated using: the ideal probability values, $P_{i,ideal}$ (i.e., $P_{i,ideal}$ = 0 and 1 for Class 0 and Class 1 respectively), and the predicted probability values using the developed model, $P_{i,precicted}$, by:

$$RMSE = \sqrt{\frac{1}{n}\sum_{i=1}^{n}(P_{i,predicted} - P_{i,ideal})^2}$$
$$MAE = \frac{1}{n}\sum_{i=1}^{n}\left|P_{i,predicted} - P_{i,ideal}\right| \quad (5)$$

Table 1 summarizes these two performance metrics for each class. As shown, the *RMSE* and *MAE* values are very close for Class 0 and 1, meaning that the model is not predicting the probability values in a biased manner and in favor of one class, and the performance is comparable for both classes.

Table 2. Performance of the logistic regression model considering both classes

Class	Probability *RMSE*	Probability *MAE*
0	0.402	0.314

1	0.388	0.314

The predicted probability values shown in Figure 8 can be assigned to Class 0 and 1 by using a threshold value. A commonly used threshold value for classification is 0.5, as such the probability values in ranges (0, 0.5) and (0.5, 1) being classified as Class 0 and Class 1, respectively. Consequently, the accuracy of the predicted model can be quantified. Figure 8 shows the Receiver Operating Characteristic (ROC) curve for the developed model, which is a graphical representation used to evaluate the performance of a binary classification model. It shows the trade-off between True Positive Rate (TPR) and False Positive Rate (FPR) values at various threshold assumptions. A perfect model would result in an ROC curve passing through the top-left corner, i.e., $TPR = 1$ and $FPR = 0$. The threshold value can be selected subjectively, depending on whether higher *TPR* or lower *FPR* is desirable. For example, three threshold values, *T*, are shown on Figure 8, where threshold of 0.3 results in higher *TPR* and higher *FPR* while a threshold of 0.7 results in lower *TPR* and *FPR*.

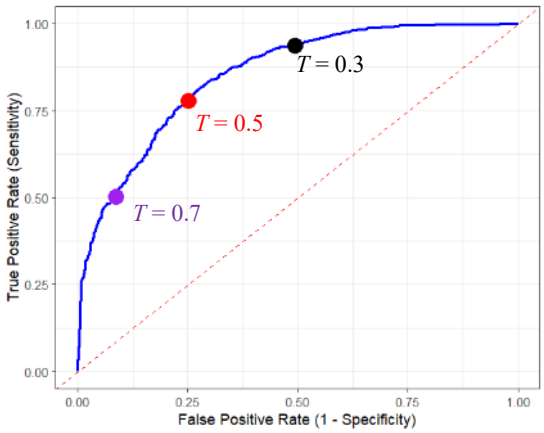

Figure 8. Predicted probability of having defect in the 2nd inspection

The Area Under the Curve (*AUC*) also quantifies the model performance without setting a specific threshold, with a perfect model having $AUC = 1$. Generally, the higher *AUC*, the better the model performance. The *AUC* of this model is calculated to be 0.853 which is considered to be very good, given a balanced (unbiased) dataset of observations is used for model development.

Furthermore, Table 3 summarizes the values of common performance metrics of the developed logistic model, and their definitions are:

$$Accuracy = (TP + TN) / (TP + TN + FP + FN) \quad (6)$$

$$Sensitivity = TPR = TP / (TP + FN) \quad (7)$$

$$Specificity = 1 - FPR = TN / (TN + FP) \quad (8)$$

$$Precision = TP / (TP + FP) \quad (9)$$

$$F1 = 2 \times Precision \times Sensitivity / (Precision + Sensitivity) \quad (10)$$

where TP = True Positive; TN = True Negative; FP = False Positive; FN = False Negative. In Table 3, these values of these metrics are obtained by applying a threshold value of 0.5 to the prediction model, all of which are above 0.75, implying the good performance of the developed model. In addition, the confusion matrix of the developed model is shown in Table 4, considering the threshold of 0.5. It shows that 77.8% and 74.8% are correctly classified for actual Class 1 and Class 0, respectively.

Table 3. The values of performance metrics of the developed logistic model

Accuracy	*TPR*	1- *FPR*	*F1*
0.76	0.78	0.75	0.77

Table 4. Confusion matrix of the developed logistic model considering threshold of 0.5

		Predicted Class	
		0	1
Actual Class	1	244 (22.2%)	**857 (77.8%)**
	0	**824 (74.8%)**	277 (25.2%)

Test Data Error

As an established assumption in Statistics, cross validation error is considered an unbiased estimate of the error the developed model will have on new, unseen data. Table 5 and 6 summarize respectively the performance metrics and confusion matrix using a 5-fold Cross Validation (CV) technique. In this technique the data is divided into five equal subsets, each subset is used once as the test set while the model is trained on the remaining four, and the results are averaged. As can be seen, the metrics and accuracy are comparable to those mentioned in Tables 3 and 4. Therefore, it is concluded that the developed model is expected to perform on unseen data as well as it does on the training data.

Table 5. The values of performance metrics using 5-fold cross validation

Accuracy	*TPR*	*1-FPR*	*ROC*
0.73	0.81	0.75	0.82

Table 6. Confusion matrix using 5-fold cross validation considering threshold of 0.5

		Predicted Class

		0	1
Actual	1	24.8%	**75.2%**
Class	0	**70.8%**	29.2%

Project Financial Activities Incurred during the Reporting Period:

The financial charges include the professional service from inferModel, graduate student stipend, tuition and corresponding fringe benefit, and indirect cost.

Project Activities with Cost Share Partners:

Cost share has been charged as planned.

Project Activities with External Partners:

Monthly meetings were held with our external industry partner to discuss the data collected and preliminary analysis results.

Potential Project Risks:

So far no risk has been identified.

Future Project Work:

In the next quarter, the following items will be taken for Task 3:

- The experimental testing will be conducted in the next 90 days. It includes the proposed different DC interference conditions and CP levels.
- CP will be coupled with different DC interferences for X60 metal.
- X70 metal will also be studied after the study of X60 metal.
- The data analysis of these testing results will also be conducted.

For Task 4, the following activities will be conducted:

- Evaluating the effect of influencing parameters on the behavior of the logistic regression model developed for predicting the probability of corrosion occurrence
- Developing probabilistic models for predicting the parameters of the developed density estimation model using the influencing factors

Potential Impacts to Pipeline Safety:

At the current phase, the project provides a useful model for predicting the probability of corrosion defect occurrence for a joint when the latest inspection shows the joint does not have any defect. In addition, the project provides approaches to propagate the measurement errors in ILI tool to defect analysis.